

Electronic Supplementary Information (ESI)

Photoluminescence mechanisms of BF₂-formazanate dye sensitizers: A theoretical study

by

Parichart Suwannakham

Pannipa Panajapo

Phorntep Promma

Tunyawat Khrootkaew

Anyanee Kamkaew

and

*Kritsana Sagarik**

School of Chemistry

Institute of Science

Suranaree University of Technology

Nakhon Ratchasima 30000

Thailand

*corresponding author: *kritsana@sut.ac.th*

Tel./Fax: (6681) 8783994

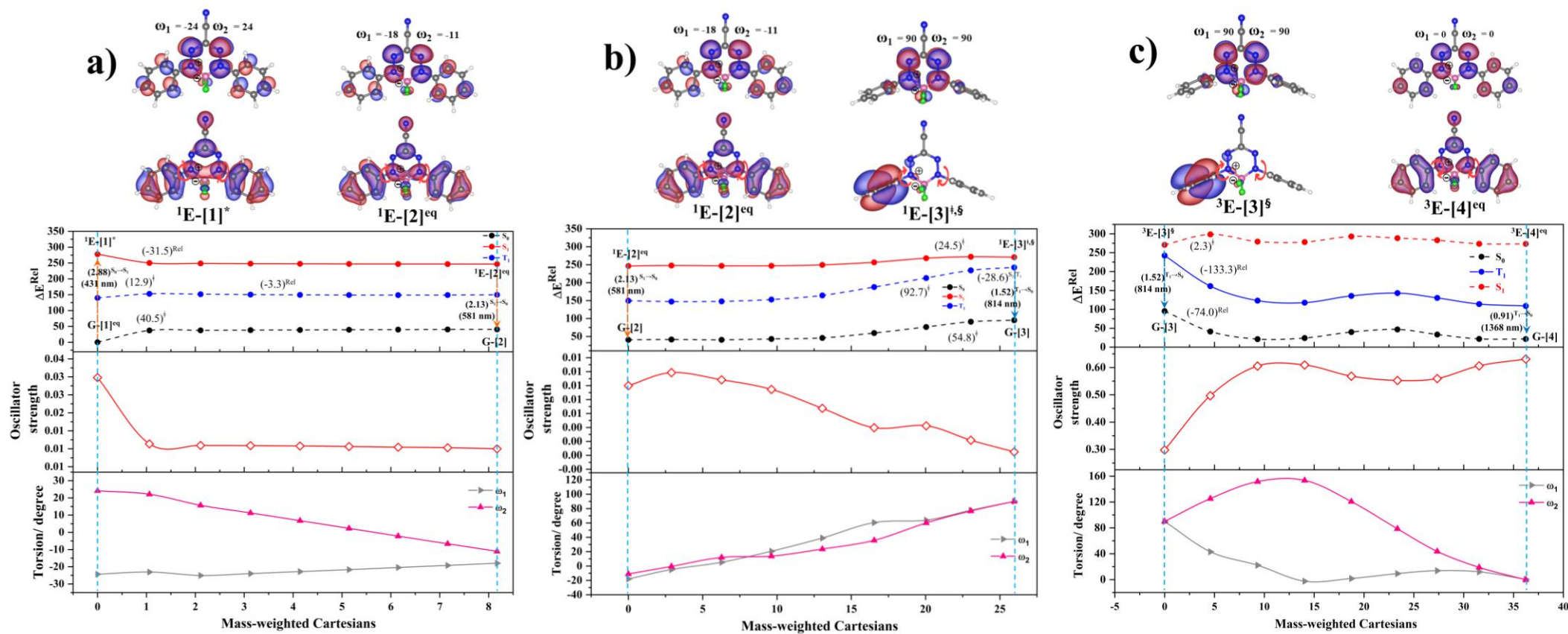


Figure S1 Potential energy surfaces for rotational motions of ω_1 and ω_2 in BF_2 -FORM, obtained based on the hypothesized pathways in Figure 4, and the DFT/B3LYP/6-311G, TD-DFT/B3LYP/6-311G, and NEB methods. Dash lines are the potential energy curves computed using the geometries on the NEB potential energy curves (solid lines). a) $(I)^* \rightarrow (II)^*$. b) $(II)^* \rightleftharpoons (III)^{\ddagger, \S}$. c) $(III)^{\ddagger, \S} \rightarrow (IV)$.

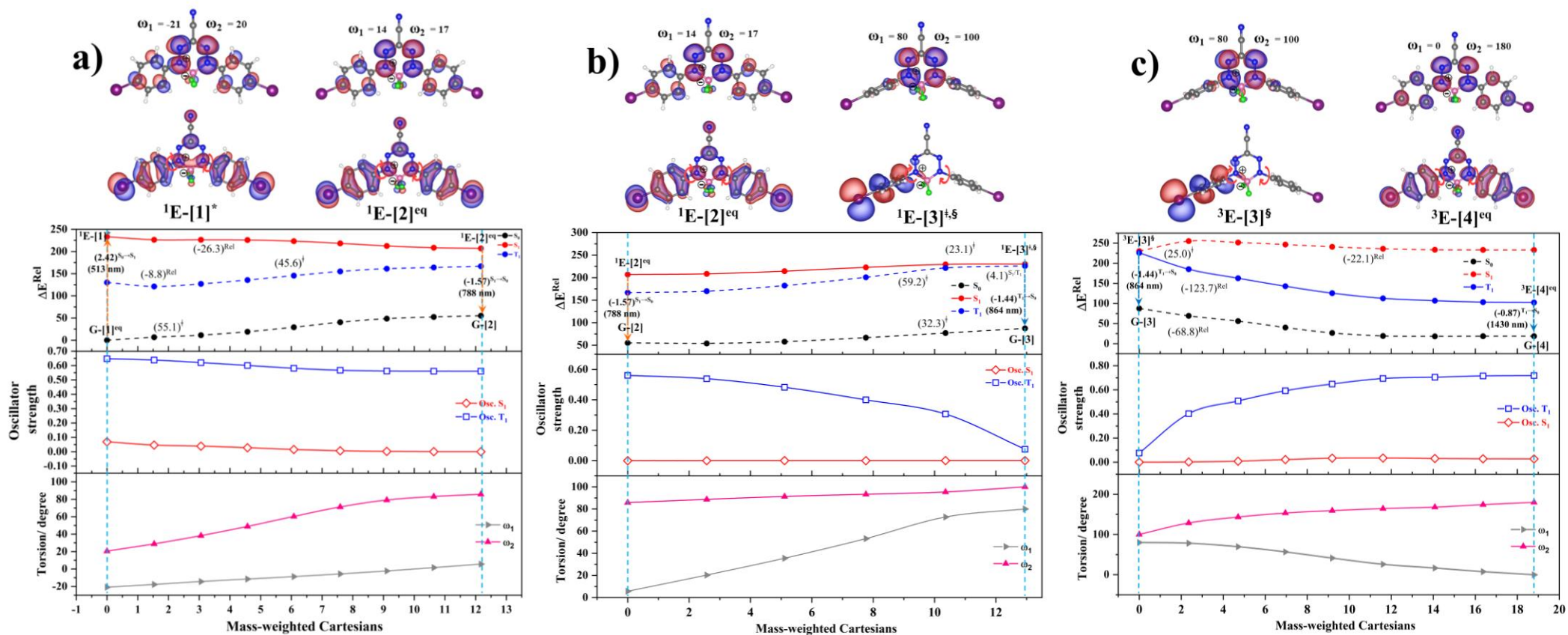
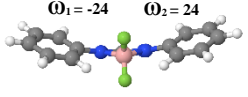
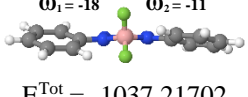
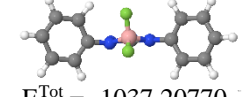
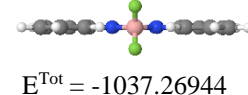


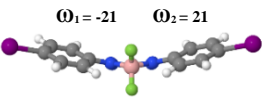
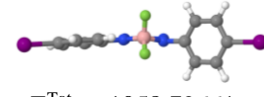
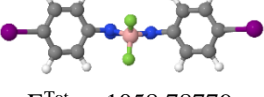
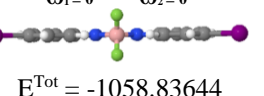
Figure S2 Potential energy surfaces for the rotational motions of ω_1 and ω_2 in BF₂-FORM-D, obtained based on the hypothesized pathways in Figure 4, and the DFT/B3LYP/6-311G, TD-DFT/B3LYP/6-311G, and NEB methods. Dash lines are the potential energy curves computed using the geometries on the NEB potential energy curves (solid lines). a) (I)^{*} → (II)^{*}. b) (II)^{*} ⇌ (III)^{‡,§}. c) (III)^{‡,§} → (IV).

Table S1 Characteristic structures and energies of BF₂-FORM in the S₀, S₁ and T₁ states obtained from DFT/B3LYP/6-311G and TD-DFT/B3LYP/6-311G calculations.

BF ₂ -FORM	TD-DFT				NX			RICC2	
	$\Delta E^{S_0 \rightarrow S_1}$	$\Delta E^{S_1 \rightarrow S_0}$	$\Delta E^{S_1 \rightarrow T_1}$	$\Delta E^{T_1 \rightarrow S_0}$	$\Delta E_{NX}^{S_0 \rightarrow S_1}$	$\Delta E_{NX}^{S_1 \rightarrow S_0}$	$\tau_{NX}^{S_1 \rightarrow S_0}$	$\Delta E_{SOC}^{T_1 \rightarrow S_0}$	$\tau_{SOC}^{T_1 \rightarrow S_0}$
G-[1]^{eq} $\omega_1 = -24$ $\omega_2 = 24$  $E^{Tot} = -1037.31086$	2.88	-	-	-	2.71	-	2.95×10^{-9}	-	-
¹E-[2]^{eq} $\omega_1 = -18$ $\omega_2 = -11$  $E^{Tot} = -1037.21702$	-	-2.13	-	-	-	-2.46	8.88×10^{-7}	-	-
¹E-[3][§] $\omega_1 = 90$ $\omega_2 = 90$  $E^{Tot} = -1037.20770$	-	-1.82	-0.30	-1.52 (P ₁)	-	-	-	-1.94 (P ₁)	0.36
³E-[4]^{eq} $\omega_1 = 0$ $\omega_2 = 0$  $E^{Tot} = -1037.26944$	-	-0.91	-	-0.91 (P ₂)	-	-0.91	1.13×10^{-6}	-1.05 (P ₂)	131

E^{Tot} = total energy in au; $\Delta E^{S_0 \rightarrow S_1}$ = excitation energy in eV; $\Delta E_{NX}^{S_0 \rightarrow S_1}$ = excitation energy obtained based on 200 Wigner sampled structures; ω_1 and ω_2 = dihedral angles defined in Figure 2; $\Delta E^{T_1 \rightarrow S_0}$ = singlet-triplet energy gap on the potential energy surface; [...] ^{eq} = equilibrium structure; [...] [§] = structure at the S₁/T₁ intersection; $\tau_{NX}^{S_1 \rightarrow S_0}$ and $\tau_{SOC}^{T_1 \rightarrow S_0}$ = fluorescence and phosphorescence lifetimes in s, respectively; $\Delta E_{SOC}^{T_1 \rightarrow S_0}$ = singlet-triplet energy gap obtained from SOC-PT-CC2/aug-cc-pVDZ calculations.

Table S2 The characteristic structures and energies of BF₂-FORM-D in the S₀, S₁ and T₁ states obtained from DFT/B3LYP/6-311G and TD-DFT/B3LYP/6-311G calculations.

BF ₂ -FORM-D	TD-DFT				NX			RICC2	
	$\Delta E^{S_0 \rightarrow S_1}$	$\Delta E^{S_1 \rightarrow S_0}$	$\Delta E^{S_1 \rightarrow T_1}$	$\Delta E^{T_1 \rightarrow S_0}$	$\Delta E_{\text{NX}}^{S_0 \rightarrow S_1}$	$\Delta E_{\text{NX}}^{S_1 \rightarrow S_0}$	$\tau_{\text{NX}}^{S_1 \rightarrow S_0}$	$\Delta E_{\text{SOC}}^{T_1 \rightarrow S_0}$	$\tau_{\text{SOC}}^{T_1 \rightarrow S_0}$
G-[1]^{eq} $\omega_1 = -21$ $\omega_2 = 21$  $E^{\text{Tot}} = -1058.87541$	2.42	-	-	-	2.32	-	3.94×10^{-9}	-	-
¹E-[2]^{eq} $\omega_1 = 5$ $\omega_2 = 86$  $E^{\text{Tot}} = -1058.79661$	-	-1.57	-	-	-	-1.65	8.49×10^{-7}	-	-
¹E-[3][§] $\omega_1 = 80$ $\omega_2 = 100$  $E^{\text{Tot}} = -1058.78779$	-	-1.48	-0.04	-1.43 (P ₁)	-	-	-	-1.93 (P ₁)	0.33
³E-[4]^{eq} $\omega_1 = 0$ $\omega_2 = 0$  $E^{\text{Tot}} = -1058.83644$	-	-0.88	-	-0.87 (P ₂)	-	-0.94	5.20×10^{-8}	-0.98 (P ₂)	194

E^{Tot} = total energy in au; $\Delta E^{S_0 \rightarrow S_1}$ = excitation energy in eV; $\Delta E_{\text{NX}}^{S_0 \rightarrow S_1}$ = excitation energy obtained based on 200 Wigner sampled structures; ω_1 and ω_2 = dihedral angles defined in Figure 2; $\Delta E^{T_1 \rightarrow S_0}$ = singlet-triplet energy gap on the potential energy surface; [...] ^{eq} = equilibrium structure; [...] [§] = structure at the S₁/T₁ intersection; $\tau_{\text{NX}}^{S_1 \rightarrow S_0}$ and $\tau_{\text{SOC}}^{T_1 \rightarrow S_0}$ = fluorescence and phosphorescence lifetimes in s, respectively; $\Delta E_{\text{SOC}}^{T_1 \rightarrow S_0}$ = singlet-triplet energy gap obtained from SOC-PT-CC2/aug-cc-pVDZ calculations.

Table S3 Thermodynamics and kinetics of the photoluminescence pathway (Figure 4) for BF₂-FORM. Rate constants, temperatures and energies are in s⁻¹, K and kJ/mol, respectively; ΔE^\ddagger = energy barrier; $\Delta E^{\ddagger, \text{ZPC}}$ = zero-point energy-corrected barrier, obtained by including the zero-point correction energy to the energy barrier obtained from the NEB method (ΔE^\ddagger); ΔH^\ddagger = activation enthalpy; ΔS^\ddagger = activation entropy; ΔG^\ddagger = activation Gibbs free energies; T_c = crossover temperature; T = temperature; $k_{f/r}^{\text{Q-vib}}$ = rate constant obtained with quantized vibrations including the zero-point vibrational energy; f/r = forward or reverse direction.

Table S3

Reaction Pathway	ΔE^\ddagger	$\Delta E^{\ddagger,ZPC}$	ΔH^\ddagger	T_c	T	$k_{f/r}^{Q-vib}$	ΔG^\ddagger	ΔS^\ddagger
${}^1E-[1]^* \leftarrow {}^1E-[2]^{eq}$	31.5	20.3	23.8	372	300	3.24×10^9	18.87	1.63×10^{-2}
					330	7.51×10^9	18.71	1.53×10^{-2}
					413	4.18×10^{10}	18.27	1.34×10^{-2}
					550	2.47×10^{11}	17.55	1.13×10^{-2}
${}^1E-[2]^{eq} \rightarrow {}^1E-[3]^{\ddagger,\S}$	24.4	20.7	21.8	5	300	5.85×10^8	23.14	-4.51×10^{-3}
					330	1.29×10^9	23.55	-5.36×10^{-3}
					413	6.27×10^9	24.78	-7.25×10^{-3}
					550	3.10×10^{10}	27.03	-9.54×10^{-3}
${}^3E-[3]^\S \leftarrow {}^3E-[4]^{eq}$	133.3	127.1	129.3	42	300	5.26×10^{-10}	126.78	8.40×10^{-3}
					330	5.79×10^{-8}	126.82	7.51×10^{-3}
					413	7.13×10^{-4}	126.99	5.60×10^{-3}
					550	9.03×10^0	127.45	3.38×10^{-3}

Table S4 Thermodynamics and kinetics of the photoluminescence pathway (Figure 4) for BF₂-FORM-D. Rate constants, temperatures and energies are in s⁻¹, K and kJ/mol, respectively; ΔE^\ddagger = energy barrier; $\Delta E^{\ddagger, \text{ZPC}}$ = zero-point energy-corrected barrier, obtained by including the zero-point correction energy to the energy barrier obtained from the NEB method (ΔE^\ddagger); ΔH^\ddagger = activation enthalpy; ΔS^\ddagger = activation entropy; ΔG^\ddagger = activation Gibbs free energies; T_c = crossover temperature; T = temperature; $k_{f/r}^{\text{Q-vib}}$ = rate constant obtained with quantized vibrations including the zero-point vibrational energy; f/r = forward or reverse direction.

Table S4

Reaction Pathway	ΔE^\ddagger	$\Delta E^{\ddagger,ZPC}$	ΔH^\ddagger	T_c	T	$k_{f/r}^{Q-vib}$	ΔG^\ddagger	ΔS^\ddagger
${}^1E-[1]^* \leftarrow {}^1E-[2]^{eq}$	26.3	32.9	30.4	4	300	2.26×10^4	48.49	-6.03×10^{-2}
					330	6.92×10^4	50.52	-6.10×10^{-2}
					413	6.40×10^5	56.29	-6.28×10^{-2}
					550	5.74×10^6	66.34	-6.53×10^{-2}
${}^1E-[2]^{eq} \rightarrow {}^1E-[3]^{\ddagger,\S}$	23.1	30.0	26.9	4	300	2.45×10^4	48.29	-7.12×10^{-2}
					330	6.64×10^4	50.64	-7.18×10^{-2}
					413	4.78×10^5	57.29	-7.36×10^{-2}
					550	3.31×10^6	68.86	-7.62×10^{-2}
${}^3E-[3]^\S \leftarrow {}^3E-[4]^{eq}$	123.7	118.7	120.7	134	300	1.08×10^{-8}	119.25	4.74×10^{-3}
					330	8.68×10^{-7}	119.40	3.87×10^{-3}
					413	5.70×10^{-3}	120.86	1.97×10^{-3}
					550	3.84×10^1	120.83	-2.81×10^{-4}